Archives of Gerontology and Geriatrics 62 (2016) 125–132

Contents lists available at ScienceDirect

Archives of Gerontology and Geriatrics

journal homepage: www.elsevier.com/locate/archger

Default mode network connectivity is linked to cognitive functioning and CSF $A\beta_{1-42}$ levels in Alzheimer's disease

Ozlem Celebi[a], Andac Uzdogan[b], Kader Karli Oguz[c], Arzu Ceylan Has[d], Anil Dolgun[e], Gul Yalcin Cakmakli[a], Filiz Akbiyik[b], Bulent Elibol[f], Esen Saka[f,*]

[a] Hacettepe University, Institute of Health Sciences, Department of Neurological Sciences and Psychiatry, Ankara, Turkey
[b] Hacettepe University Faculty of Medicine, Department of Medical Biochemistry, Ankara, Turkey
[c] Hacettepe University Faculty of Medicine, Department of Radiology, Ankara, Turkey
[d] Bilkent University, National Magnetic Resonance Research Center, Ankara, Turkey
[e] Hacettepe University Faculty of Medicine, Department of Biostatistics, Ankara, Turkey
[f] Hacettepe University Faculty of Medicine, Department of Neurology, Ankara, Turkey

ARTICLE INFO

Article history:
Received 11 May 2015
Received in revised form 25 September 2015
Accepted 28 September 2015
Available online 17 October 2015

Keywords:
Alzheimer's disease
Biomarker
Cognition
Resting functional magnetic resonance imaging
Posterior cingulate cortex
Retrosplenial cortex

ABSTRACT

Background: Changes in the default mode network (DMN) activity are early features of Alzheimer's disease (AD) and may be linked to AD-specific Aβ pathology.
Methods: Cognitive profiles; DMN connectivity alterations; and cerebrospinal fluid (CSF) amyloid beta $(A\beta)_{1-42}$, total tau, phosphorylated tau 181, and α-synuclein levels were studied in 21 patients with AD and 10 controls.
Results: DMN activity is altered in AD. Posterior cingulate cortex (PCC) functional connectivity with other parts of DMN was related to cognitive function scores. The reduction of connectivity of the dorsal PCC with the retrosplenial cortex on the right side was closely related to decreased CSF $A\beta_{1-42}$ levels in patients with AD.
Conclusions: The dorsal PCC and retrosplenial cortex may have special importance in the pathogenesis and cognitive findings of AD.

1. Introduction

Alzheimer's disease (AD) is the most common neurodegenerative disease, which is characterized by distinct clinical features, pathology, and pathogenesis. An early diagnosis of AD can be made using well-established biomarkers and imaging markers. These markers are expected to be the rational use of therapeutics for halting the progression of the AD-specific pathophysiological cascade and thus preventing Alzheimer's dementia. Concomitant with this idea, increasing efforts have been made to find new markers and to improve the existing ones used for AD and other neurodegenerative disorders.

A proposed model of the AD pathophysiological cascade suggests that the initial detectable pathophysiological change in AD is the accumulation of amyloid beta (Aβ) in the brain (Hardy, 1992; Selkoe, 2002). Accordingly, the detection of Aβ deposition on positron emission tomography (PET) and decreased cerebrospinal fluid (CSF) Aβ levels are expected to be the earliest signs for diagnosing AD in vivo (Blennow, Zetterberg, & Fagan, 2012; Sperling et al., 2011). Measures of synaptic dysfunction, such as a regional decrease in glucose metabolism, demonstrated by fluorodeoxyglucose (FDG) PET and altered connectivity patterns in functional magnetic resonance imaging (fMRI) closely follow these Aβ changes. Likewise, specific alterations in resting-state networks, in particular changes in the default mode network (DMN), are evident in prodromal AD. On the other hand, the elevated CSF total-tau (t-tau) and phosphorylated tau 181 ($p\text{-}tau_{181}$) levels are believed to be indicators of neuronal injury. Therefore, they occur relatively later in the development of AD pathology (Blennow et al., 2012).

Resting-state networks are active during rest and can be either task positive or task negative (Rektorova, 2014). DMN is a task-negative network measured by resting-state fMRI. It is closely related to higher cognitive functions and is largely believed to reflect the transit of early disease-specific molecular alterations to evident neurodegeneration in degenerative diseases such as AD (Barkhof, Haller, & Rombouts, 2014). It has already been shown that resting-state networks, such as DMN and the central executive network, are altered in AD (Gour et al., 2014; Hahn et al., 2013).

* Corresponding author. Hacettepe University Faculty of Medicine, Department of Neurology, Ankara 06100, Turkey.
E-mail address: esensaka@hacettepe.edu.tr (E. Saka).

http://dx.doi.org/10.1016/j.archger.2015.09.010
0167-4943/

DMN is the most extensively studied resting-state network, revealing similar altered patterns of functional connectivity (FC) in patients with both sporadic and autosomal dominant AD (ADAD). Several studies have also analyzed the validity of DMN activity changes in diagnosing AD and reported a specificity and sensitivity of 70–80% (Balthazar, de Campos, Franco, Damasceno, & Cendes, 2014; Koch et al., 2012; Li et al., 2012). The disruption of DMN has been demonstrated as a very early feature in AD; even the asymptomatic carriers of ADAD mutations and individuals at risk of AD, such as patients with mild cognitive impairment, elderly carriers of ApoEε4, and cognitively normal patients with PET demonstrating Aβ deposition, experience decreases in the DMN connectivity (Chhatwal et al., 2013; Elman et al., 2014; Jack et al., 2013; Koch et al., 2014; Sperling et al., 2009).

The National Institute on Aging and the Alzheimer's Association (NIA-AA) recently established a revised diagnostic criteria for AD dementia (McKhann et al., 2011) and recommended the use of CSF biomarkers, such as decreased CSF $A\beta_{1-42}$ levels and elevated CSF t-tau and p-tau_{181} levels, in addition to PET or magnetic resonance imaging (MRI), for detecting AD, when there is a need to confirm that the dementia syndrome is caused by AD. There are a considerable number of studies comparing or combining different biomarkers for diagnosing AD, although there are only a few studies that analyze both DMN connectivity and CSF biomarkers and their relationship in AD (Wang et al., 2013; Li et al., 2013; Sheline et al., 2010). In the present study, we hypothesized that the biomarkers of AD in different modalities (i.e., protein markers and imaging markers) and the magnitude of clinical dysfunction are related if the proposed model of the AD pathophysiological cascade was valid. Furthermore, finding a significant correlation between the well-established CSF biomarkers and changes in DMN activity, particularly in the specific regions of the brain, could increase the diagnostic utility of DMN activity studies in AD. Therefore, in the present study, we analyzed the CSF $A\beta_{1-42}$, t-tau, and p-tau_{181} levels as well-known biomarkers of AD pathology as well as the CSF α-synuclein levels as another marker of synaptic and/or neuronal injury in a group of newly diagnosed patients with AD in comparison with the controls. DMN activity and cognitive profiles of the same subjects were also comparatively examined in relation to these biomarkers.

2. Methods

2.1. Subjects and clinical assessment

Twenty-one patients with probable AD and 10 age-matched healthy controls participated in the present study. Written informed consent was obtained from all participants and/or a family member. The study was approved by the Ankara University Faculty of Medicine Ethical Board for Clinical Studies. The clinical diagnosis of AD was based on the National Institute of Neurological and Communicative Disorders and Stroke–Alzheimer's Disease and Related Disorders Association criteria (McKhann et al., 1984, 2011). Patients with AD were prospectively recruited from the Neurology outpatient clinics at the Hacettepe University Hospitals between September 2012 and June 2014. Controls were recruited from the community. Healthy controls had no cognitive complaints or a history of neurological disease. The mini-mental state examination (MMSE), geriatric depression scale (GDS), and a neuropsychological test battery, including enhanced cued recall, semantic fluency, phonemic fluency, trail making test A and B, reciting months backwards, and clock drawing tests (evaluated according to a 4-point scoring system), were administered to all subjects. The administration and scoring of these tests were as previously described (Cangoz, Karakoc, & Selekler, 2006; Celebi, Temucin, Elibol, & Saka, 2014; Saka, Mihci, Topcuoglu, & Balkan, 2006). Clinical assessment, MRI data acquisition, and CSF collection (only for patients with AD) were performed within a 1-week period in each subject.

2.2. CSF collection and analysis of biomarkers

CSF was collected according to new consensus-based recommendations for preanalytical issues with AD and Parkinson's disease (PD) CSF biomarker analysis (del Campo et al., 2012). In brief, atraumatic lumbar puncture was performed using a 22-gauge needle in the L4–5 or L3–4 intervertebral space to remove 12 mL CSF. No serious adverse event was reported. CSF samples were centrifuged at $2000 \times g$ for 10 min within 30 min of collection. Samples were aliquoted into 0.5-mL polypropylene storage tubes and stored in a −80 °C freezer until analysis. All archived samples were analyzed at the Clinical Biochemistry Laboratory at Hacettepe University Hospitals.

CSF $A\beta_{1-42}$, t-tau, and p-tau_{181} levels were analyzed using plate-based enzyme-linked immunosorbent assay (ELISA) (INNOTEST; Innogenetics, Ghent, Belgium). CSF α-synuclein was measured using ELISA (catalog no. SIG 38974; Covance, Dedham, MA) according to the manufacturer's instructions. CSF hemoglobin levels were also determined to evaluate blood contamination and to control the possible confounding effect of hemolysis on the CSF α-synuclein level. CSF hemoglobin was analyzed using the ELISA method with reagents obtained from Bethyl Laboratories according to the manufacturer's instructions. CSF protein concentrations were determined using a colorimetric method by Beckman Coulter analyzers.

2.3. Imaging methods

2.3.1. Data acquisition and preprocessing

All imaging data of the brain were obtained on a 3T MR scanner (Magnetom, Trio TIM system; Siemens, Germany) equipped with an 8-channel phased-array head coil. A T2*-weighted gradient-echo spiral pulse sequence (repetition time [TR] 2000 ms; time to echo [TE], 30 ms; flip angle, 80°) was used for the resting-state functional scans. It comprised 150 dynamic series that required 5 min. The field of view (FOV) was $230 \times 230\ mm^2$, and the matrix size was 64×64, giving an in-plane spatial resolution of 3.6 mm. The subjects kept their eyes closed and remained still without concentrating on anything specific. For anatomical data, all subjects also underwent structural T1-weighted three-dimensional (3D) high-resolution images with 0.9-mm isotropic voxels [magnetization-prepared rapid gradient-echo-(MPRAGE)] (TR/TE: 1900/3.4 ms; FA: 90; FOV: 256 mm; matrix: 224×256; distance factor: 50%).

Data were preprocessed using SPM8 software (Statistical Parametric Mapping SPM Software, 2015). Motion correction using least-squares minimization without higher-order corrections for spin history and normalization (Friston et al., 1995) of both functional and structural 3D T1-weighted MPRAGE data to the Montreal Neurological Institute (MNI) template were performed. Images were then resampled every 2-mm isotropic voxel size using sinc interpolation and smoothed with a 4-mm full width at half maximum (FWHM) Gaussian kernel to decrease the spatial noise. Resampling and smoothing were done in three dimensions yielding a 2-mm^3 resolution and effective spatial smoothness (FWHM) of $7.2 \times 7.1 \times 8.4$ mm. Normalized data of each subject were used as input for MELODIC independent component analysis (Beckmann & Smith, 2004) for identifying and removing noise components. Temporal filtering was applied using both high-pass (Gaussian-weighted least-squares straight line fitting, with sigma = 100.0 s) and low-pass filters (Gaussian low-pass temporal filtering: half-width at half-maximum, 2.8 s).

We performed individual seed-based connectivity for the analysis of FC in individuals and analysis of the seed-voxel group for building a composite map for the entire group of similar subjects in Fig. 2. All of the presented data, except the data in Fig. 2, are the results of individual seed-based connectivity analysis.

2.3.2. FC analysis (individual seed-based connectivity)

For individual seed-based connectivity, FMRIB's Software Library (www.fmrib.ox.ac.uk/fsl) (FSL, 2015) was used to examine functional coupling respectively between the posterior cingulate cortex (PCC), left dorsal PCC, right dorsal PCC, left ventral PCC, right ventral PCC (Supplementary Table 1), and seven other regions of interest (ROI) (Supplementary Table 2) located in DMN regions during the resting state. Each subject's time series was transformed into MNI space using 12° of freedom linear affine transformation implemented in FLIRT (voxel size = $1 \times 1 \times 1$ mm) to obtain the time series for each seed, for each subject. ROI was defined as spheres with a 6-mm radius. To form a sphere mask around a voxel of interest, the fslmaths commands were used. The mean time series was extracted from a normalized and transformed fMRI for all of the sphere-masked voxels using the fslmeants command. The FEAT toolbox (FEAT, 2015) was used with the seed time series file that was just created to perform multiple regression analyses (Di et al., 2008). To extract the unique variance that the time series for each seed mask reflects, time series for each seed were orthogonalized with respect to each other using the Gram–Schmidt process. Individual subject-level maps of all positively and negatively predicted voxels for each regressor were created by this analysis, and *Z*-score values were calculated for each subject (Margulies et al., 2007).

2.3.3. FC analysis (seed-voxel group analysis)

Using the CONN toolbox in MATLAB R2008a (www.nitrc.org/projects/conn), principal components associated with segmented white matter and CSF for each subject were identified, and white matter, CSF, and realignment parameters were entered as confounders in a first-level analysis. The data were band-pass filtered to 0.008–0.09 Hz. For a group analysis, seed-voxel analysis was then used, and connectivity patterns were separately specified for five 6-mm spherical clusters; five seed ROI located in PCC, the left dorsal PCC, the right dorsal PCC, the left ventral PCC, and the right ventral PCC. Using the specified five seed ROI, temporal correlations were computed between these seeds and all other voxels in the brain. Seed-to-voxel results were reported as significant at a voxel-wise threshold level of $p < 0.001$ uncorrected and a cluster-level threshold of $p < 0.05$ corrected for the false discovery rate (FDR). The *t*-test and Fisher's Z-transformed correlations were used to compute differences in FC between the patients with AD and healthy controls.

2.4. Statistical analysis

Mean ± standard error of the mean values are used to describe the quantitative variables. Frequencies and percentages are given for nominal data. Normality assumption was checked using the Shapiro–Wilk test. Independent samples t test and Mann–Whitney *U* test were used to compare the groups in terms of quantitative variables. The sex distribution among the study groups was analyzed using Fisher's exact test. An exploratory factor analysis (using principal component analysis for factor extraction) was applied to combine several quantitative variables into a single factor to reduce high-dimensional data. Accordingly, PCC (the connectivity of PCC with the other nodes of the DMN), ventral PCC (the connectivity of the right and left ventral PCC with the other nodes of DMN), dorsal PCC (the connectivity of the right and left dorsal PCC with the other nodes of the DMN), memory (enhanced cued recall and semantic fluency), and executive function (trial making B, reciting months backwards, and verbal fluency) factors were built. For all extracted factors, explained variances were more than 50% with a single factor. The nonparametric Spearman correlation analysis (without applying any covariate adjustment) was then used to analyze the relationship between both the quantitative variables and extracted factors. The FDR control was applied for all analyses to correct for multiple comparisons (Benjamini & Hochberg, 1995). IBM-SPSS version 21.0 (IBM Corp., Armonk, NY) and R package "p.adjust" (R Core Team, 2013) version 3.0.2 (The R Foundation for Statistical Computing) were used, and the statistical significance was set at $p < 0.05$.

3. Results

3.1. Demographics and cognitive profile

The demographics and cognitive features of subjects are summarized in Table 1. Patients with AD and controls were matched for age, education, and sex. In patients with AD, disease severity was mild to moderate, with a mean MMSE score of 18.1 ± 1.4, whereas the mean MMSE score of the control group was 27.5 ± 0.7. The performance of patients with AD was lower than that of the controls in all of the neuropsychological tests administered (all *p* values <0.05). The GDS score was higher in patients with AD than controls ($p = 0.025$).

3.2. CSF biomarkers

CSF $A\beta_{1-42}$, t-tau, p-tau_{181}, and α-synuclein levels and ratio of α-synuclein to total protein in patients with AD are presented in Table 2. These values were compared with another group of control subjects ($n = 24$) who underwent diagnostic lumbar puncture for headache or peripheral nervous system disorders. None of them had neurodegenerative disease. As expected, patients with AD had a lower CSF $A\beta_{1-42}$ and higher CSF t-tau and p-tau_{181} levels than controls ($p < 0.05$). Patients with AD had higher CSF α-synuclein levels than controls (2035.2 ± 266.5 vs. 1425.9 ± 182.5 pg/mL, respectively; $p < 0.05$) as well as a higher ratio of α-synuclein to total protein (51.8 ± 6.5 vs. 35.5 ± 4.7; $p < 0.05$). This ratio correlated with the level of p-tau_{181} in patients with AD.

Table 1
The demographics and the cognitive features of the subjects with AD and controls.

	AD (21)	Control (10)	*p* Value*
	mean ± SEM	mean ± SEM	
Age (yrs)	66.4 ± 1.9	66.6 ± 2.3	0.852
Education (yrs)	9.3 ± 1.3	10.3 ± 1.3	0.917
Gender (F/M)	8/13	8/2	0.054
Disease duration (yrs)	2.8 ± 0.3	–	N/A
MMSE (range)	18.1 ± 1.4 (11-23)	27.5 ± 0.7 (24-30)	0.002
ECR	16.2 ± 2.9	46.1 ± 0.7	0.002
Semantic fluency	8.4 ± 0.7	15.7 ± 1.2	0.002
Verbal fluency	5.7 ± 1.0	9.7 ± 1.5	0.028
Trail making A	165.6 ± 25.3	66.8 ± 9.6	0.024
Trail making B	293.4 ± 16.3	144.0 ± 26.0	0.002
Reciting months backwards	167.8 ± 28.6	80.9 ± 37.1	0.024
Clock drawing test	2.2 ± 0.4	3.8 ± 0.1	0.024
GDS	4.4 ± 1.1	1.5 ± 0.5	0.025

AD, Alzheimer's disease; MMSE, mini-mental state examination; ECR, enhanced cued recall test; GDS, geriatric depression scale; SEM, standard error of mean.
* Adjusted *p* values according to the False Discovery Rate (FDR); N/A, statistical analysis is not available.

Table 2
CSF biomarkers, results of the subjects with AD and controls.

	AD ($n=21$) Mean ± SEM	Control ($n=24$) Mean ± SEM	p Value
$A\beta_{1-42}$ (pg/ml)	772.3 ± 64.5	1089.2 ± 44.8	<0.0001
t-tau (pg/ml)	681.2 ± 60.5	278.6 ± 31.4	<0.0001
p-$tau_{181,}$ (pg/ml)	90.6 ± 6.5	41.6 ± 3.9	<0.0001
α-Synuclein (pg/ml)	2035.2 ± 266.5	1425.9 ± 182.5	0.047
α-Synuclein to total protein, ratio	51.8 ± 6.5	35.5 ± 4.7	0.047

AD, Alzheimer's disease; SEM, standard error of mean.

3.3. Correlation of cognitive test performances and CSF biomarkers

The cognitive test results were not related to any of the AD-related CSF biomarkers ($A\beta_{1-42}$, t-tau, and p-tau_{181}) or α-synuclein levels.

3.4. Comparison of DMN FC across groups

We used individual seed-based connectivity analysis for the comparison of DMN FC across groups. A DMN connectivity map derived from PCC (PCC as a whole and dorsal PCC and ventral PCC separately on both sides) showed decreased FC with the medial prefrontal cortex, medial temporal lobes, inferior parietal lobules, and retrosplenial cortices in patients with AD relative to age-matched controls (Fig. 1; $p < 0.05$). We also performed seed-voxel group analysis for the visual comparison of AD and healthy control groups (Fig. 2).

3.5. Correlation of DMN integrity changes with cognitive functions

Data derived from individual seed-based connectivity analyses were used for correlation studies. Patients with AD and healthy controls were analyzed as a whole. To avoid multiple comparisons, the connectivity of PCC with the other nodes of DMN as a single unit (the PCC factor, which was extracted using factor analysis) was analyzed. We also classified neuropsychological test scores into four cognitive domains: memory (enhanced cued recall and semantic fluency), visuospatial (clock drawing), attention (trial making A), and executive functions (trial making B, reciting months backwards, and verbal fluency) and asked whether the PCC factor was related to the cognitive performance of study subjects. This analysis showed that the PCC factor was related to the MMSE score ($r = 0.546$, $p = 0.001$), attention ($r = -0.392$, $p = 0.029$), executive function factor ($r = -0.429$, $p = 0.016$), GDS score ($r = -0.522$, $p = 0.003$), and more prominently with memory factor ($r = 0.647$, $p = 0.0001$) (Table 3).

The results of further correlation analyses of PCC connectivity with the other nodes of DMN separately and individual cognitive test scores are summarized in Table 4. This analysis demonstrated the presence of significant correlations between individual cognitive test scores and connectivity of their functionally related DMN nodes with PCC.

3.6. Correlation of DMN integrity changes with CSF biomarkers

Data derived from individual seed-based connectivity analyses were used for correlation studies. Because CSF biomarkers were not studied in healthy controls, this analysis was conducted only in patients with AD. We first analyzed whether PCC connectivity as a whole (PCC factor) was related to any of the CSF markers of AD and found that CSF $A\beta_{1-42}$ levels tended to correlate with the level of connectivity of PCC, although this did not reach statistical significance ($r = 0.421$, $p = 0.058$).

Next, we sought the level of connectivity of the dorsal and ventral PCC with each DMN node individually. This analysis showed that among other DMN nodes, the connectivity of the dorsal PCC with the retrosplenial cortex on the right side was significantly related to CSF $A\beta_{1-42}$ levels ($r = 0.499$, $p = 0.021$). This finding shows that the amount of decrease of $A\beta_{1-42}$ in CSF is related to a decrease in dorsal PCC and retrosplenial cortex connectivity.

4. Discussion

In the present study, we showed that, in a resting state, the connectivity of PCC with the medial prefrontal cortex, medial temporal lobes, inferior parietal lobules, and retrosplenial cortices is decreased in patients with newly diagnosed mild to moderate AD. As expected, these patients had a lower CSF $A\beta_{1-42}$ and higher CSF t-tau and p-tau_{181} levels than controls. We additionally found that CSF α-synuclein levels were increased in these patients. The comparative analysis of all these biological and imaging parameters together with cognitive profiling depicted some expected as well as novel findings. When patients with AD and healthy controls were analyzed as a whole, the scores of cognitive functions, such as attention, executive functions, and more prominently memory domains, were related to the magnitude of PCC connectivity with other parts of DMN. Moreover, as a novel finding, in DMN, decreased connectivity of the dorsal PCC with the retrosplenial cortex was found to be closely related to decreased CSF $A\beta_{1-42}$ levels in patients with AD.

DMN includes medial temporal, frontal, and parietal cortical areas. It is active when attention is not focused but deactivates during task-related activities (Buckner, Andrews-Hanna, & Schacter, 2008). In studies of AD, changes in DMN activity particularly involved FC between PCC and hippocampus/medial temporal lobes (Greicius, Srivastava, Reiss, & Menon, 2004; Wang et al., 2013). When studying PCC connectivity, we also analyzed dorsal and ventral PCC separately because FC of the dorsal and ventral PCC may differ in the resting state and during cognitive tasks. For example, similar to the ventral PCC, the dorsal PCC has strong connectivity within DMN; however, unlike the ventral PCC, it also has connectivity to a wide range of other intrinsic connectivity networks, including frontal and parietal regions involved in cognitive control (Leech & Sharp, 2014). We found here that FC of PCC (ventral, dorsal, or total) with the other parts of DMN is altered in patients with AD. We further showed that the strength of PCC FC is lower in subjects with lower cognitive scores and higher in subjects with higher cognitive function. This finding is in accordance with previous studies that showed the alteration of PCC FC to be proportional to the severity of the disease (Chhatwal et al., 2013).

The widely accepted and largely proved pathophysiological cascade of AD suggests that altered Aβ production and its deposition is a very early step and leads to other AD-related neuronal and circuit changes (Hardy, 1992; Sperling et al., 2011). Preferentially, Aβ-deposited areas include the nodes of DMN such as PCC, retrosplenial cortex, precuneus, and parietal and temporal lobes (Wang et al., 2013; Buckner et al., 2005). Several studies have reported an association between CSF biomarkers and DMN connectivity changes (Wang et al., 2013; Li et al., 2013; Sheline et al., 2010). Among them, Wang et al. (2013) found associations of decreased CSF $A\beta_{1-42}$ levels and increased CSF p-tau levels with decreases of FC of PCC and medial temporal lobes in a large sample of cognitively normal older individuals. Li et al. (2013) showed that the ratio of $A\beta_{42}$ to p-tau181 correlated with FC within DMN in the left precuneus in AD. Based on this background, we expected changes in DMN in patients with AD to be related to Aβ deposition and CSF Aβ levels in our subjects. Indeed, we found that CSF Aβ levels were related to FC of the dorsal PCC with the retrosplenial cortex on the right side. In other

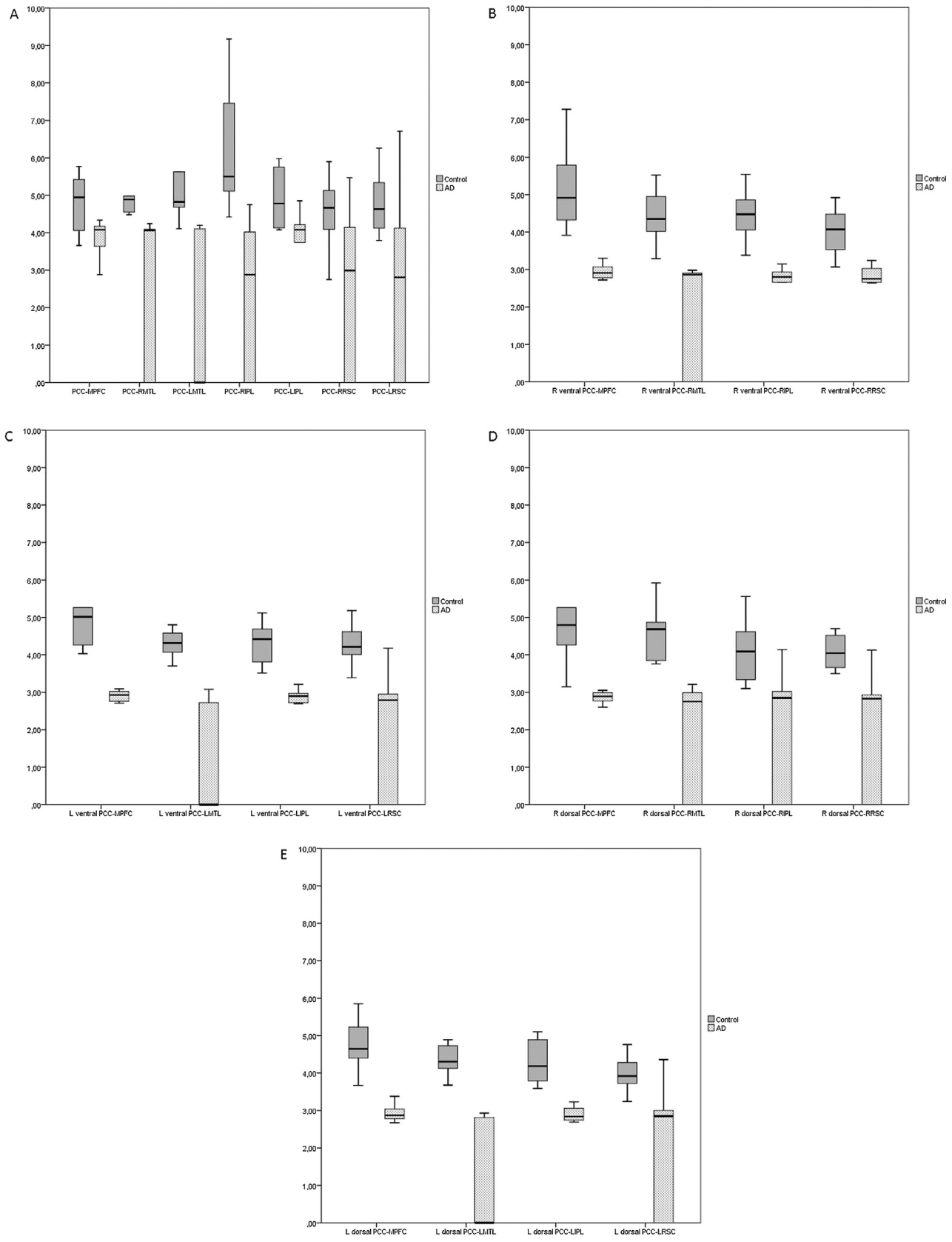

Fig. 1. Box-and-whisker plots of the functional connectivity values between (A) the posterior cingulate cortex (PCC) and the other default mode network (DMN) regions (B) right ventral PCC and the other DMN regions (C) Left ventral PCC and other DMN regions (D) right dorsal PCC and other DMN regions (E) left dorsal PCC and other DMN regions. Figure shows reduced connectivity of the PCC and ventral/dorsal PCC with the medial prefrontal cortex (MPFC), medial temporal lobes (MTL), inferior parietal lobules (IPL), and retrosplenial cortices (RSC) in Alzheimer's disease (AD) patients. $^{*}p < 0.05$, according to the False Discovery Rate (FDR) adjustment. In the Box-and-whisker plot, the box represents the values from the lower to upper quartile (the interquartile range) and the middle line represents the median of the functional connectivity values.

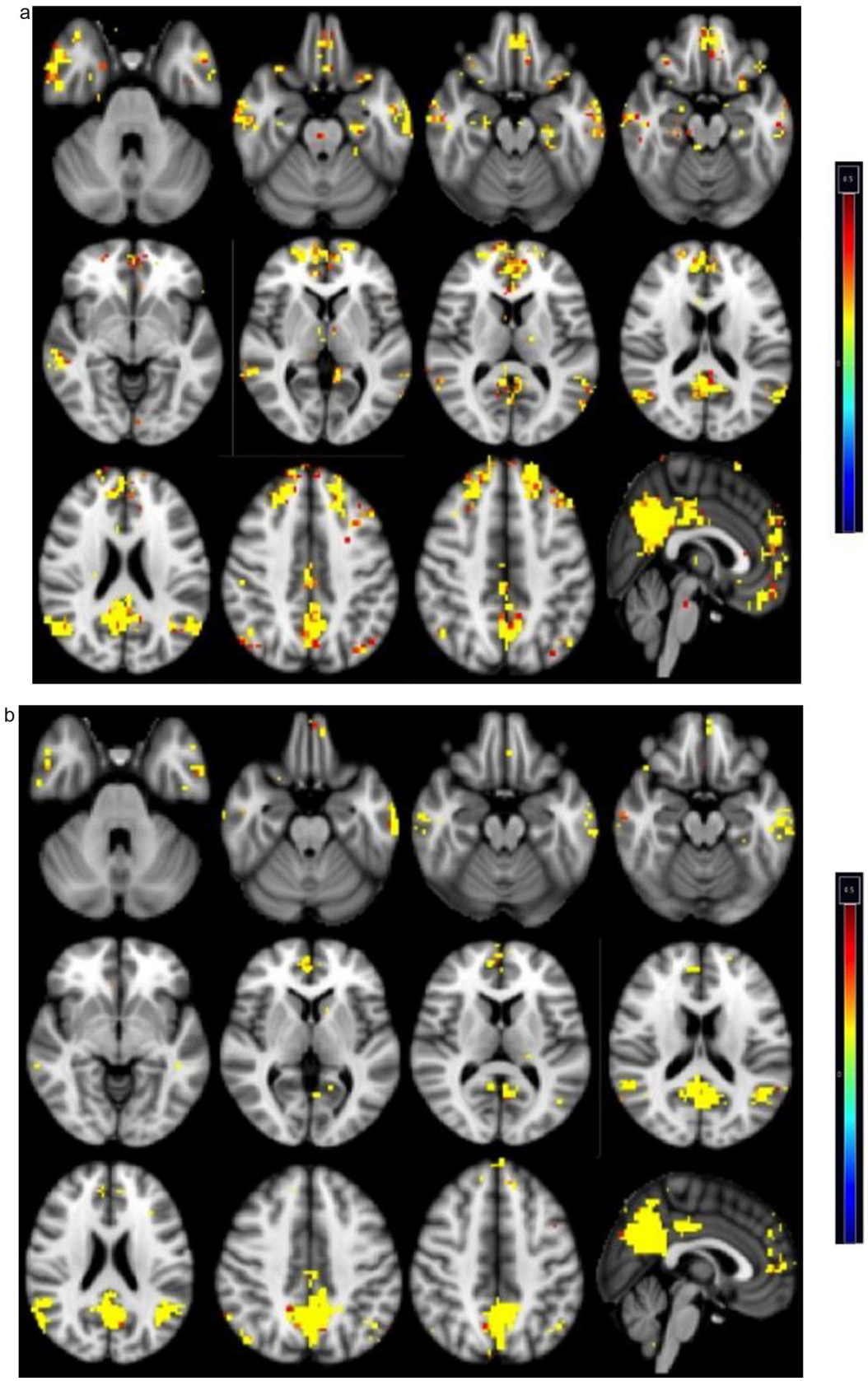

Fig. 2. Functional connectivity between the PCC and all other brain regions in the control group (A), in AD group (B). Figure shows reduced functional connectivity with medial prefrontal cortex, medial temporal lobes, inferior parietal lobules and retrosplenial cortices in AD patients relative to age-matched controls (two sided FDR $^{*}p < 0.05$, seed-level corrected $^{*}p < 0.05$).

Table 3
Correlation of the default mode network (DMN) functional connectivity (FC) values with the cognitive test scores in study subjects.

	MMSE		Memory factor		Visuo-spatial function		Attention		Executive function factor		GDS	
	r	p	r	p	r	p	r	p	r	p	r	p
PCC factor	0.55	0.001	0.65	<0.0001	0.32	NS	−0.39	0.029	−0.43	0.016	−0.52	0.003
Ventral PCC factor	0.64	<0.0001	0.69	<0.0001	0.42	0.02	−0.38	0.035	−0.50	0.004	−0.45	0.011
Dorsal PCC factor	0.58	0.001	0.66	<0.0001	0.37	0.041	−0.35	NS	−0.48	0.006	−044	0.014
PCC-R/L MTL	0.52	0.002	0.52	0.003	0.42	0.018	−0.24	NS	−0.30	NS	−0.48	0.007
R/L Dorsal PCC-R/L MTL	0.51	0.003	0.53	0.002	0.36	0.045	−0.26	NS	−0.34	NS	−0.39	0.029
R/L Ventral PCC-R/L MTL	0.51	0.003	0.55	0.001	0.36	NS	−0.22	NS	−0.33	NS	−0.40	0.026

MMSE, mini-mental state examination; GDS, geriatric depression scale; PCC, posterior cingulate cortex; R, right; L, left; MTL, medial temporal lobe; NS, non-significant; PCC factor, the connectivity of PCC with the other nodes of DMN as a single factor which is extracted by using factor analysis; Ventral PCC factor, the connectivity of R and L ventral PCC with the other nodes of DMN as a single factor which is extracted by using factor analysis; Dorsal PCC factor, the connectivity of R and L dorsal PCC with the other nodes of DMN as a single factor which is extracted by using factor analysis; Memory factor, a single factor of enhanced cued recall and semantic fluency; Executive function factor, a single factor of trial making B, reciting months backwards, verbal fluency.

Table 4
Correlation analysis of the PCC functional connectivity with the other DMN nodes and the neuropsychological test scores in the study groups.

	PCC-MPFC		PCC-RMTL		PCC-LMTL		PCC- RIPL		PCC-LIPL		PCC-RRSC		PCC-LRSC	
	r	p	r	p	r	p	r	p	r	p	r	p	r	p
MMSE	0.38	0.033	0.44	0.013	0.65	<0.0001	0.44	0.013	0.24	NS	0.44	0.012	0.33	NS
ECR	0.53	0.002	0.63	<0.0001	0.69	<0.0001	0.60	<0.0001	0.40	0.025	0.44	0.015	0.32	NS
Semantic fluency	0.29	NS	0.24	NS	0.46	0.010	0.53	0.002	0.35	NS	0.48	0.006	0.50	0.004
Verbal fluency	0.11	NS	0.002	NS	0.25	NS	0.38	0.038	0.07	NS	0.33	NS	0.11	NS
Trail making A	−0.13	NS	−0.08	NS	−0.47	0.007	−0.36	0.049	−0.07	NS	−0.49	0.006	−0.23	NS
Trail making B	−0.24	NS	−0.43	0.015	−0.62	<0.0001	−0.58	0.001	−0.17	NS	−0.45	0.011	−0.22	NS
Reciting months backwards	−0.11	NS	−0.12	NS	−0.40	0.026	−0.31	NS	−0.03	NS	−0.39	0.032	−0.32	NS
Clock drawing	0.20	NS	0.33	NS	0.52	0.003	0.24	NS	0.15	NS	0.28	NS	0.10	NS
GDS	−0.47	0.008	−0.40	0.027	−0.54	0.002	−0.34	NS	−0.27	NS	−0.16	NS	−0.28	NS

MMSE, mini-mental state examination; ECR, enhanced cued recall; GDS, geriatric depression scale; PCC, posterior cingulate cortex; R, right; L, left; MTL, medial temporal lobe; IPL, inferior parietal lobul; MPFC, medial prefrontal cortex; RSC, retrosplenial cortex.

words, in subjects with lower CSF Aβ levels, FC of the dorsal PCC with the retrosplenial cortex was lower. This finding is novel but not unexpected. Previous FDG PET studies showed decreased glucose metabolism in the very early stages of AD in PCC and the retrosplenial cortex (Buckner et al., 2005; Frings, Spehl, Weber, Hull, & Meyer, 2013). It was also shown to be associated with increased amyloid deposition and/or atrophy in these regions and the brain regions anatomically and functionally connected to them (Buckner et al., 2005; Desgranges et al., 2002; Frings et al., 2013). The retrosplenial cortex functions in spatial navigation and in acquiring new information, particularly autobiographical memory (Vann, Aggleton, & Maguire, 2009). It has connections with the hippocampal formation, parahippocampal region, and anterior and lateral dorsal thalamic nuclei as well as with PCC. Owing to those findings and others, the retrosplenial cortex in addition to PCC is believed to play a major role in cognitive deficits associated with AD (Pengas et al., 2012). The involvement of dorsal but not the ventral PCC may be because of the more deliberate use of the dorsal PCC, as it is believed to link networks that are functionally distinct but need to be coordinated for efficient cognitive processing (Leech & Sharp, 2014). Consistent with this idea, Sperling et al. found that increased Aβ deposition is associated with higher DMN activity during a memory task (Sperling et al., 2009).

Additionally, we analyzed CSF α-synuclein levels as a protein marker of synaptic degeneration not specific to AD. In fact, α-synuclein is being studied as a biomarker of PD and other α-synucleinopathies. It is decreased in PD, multiple system atrophy, and Lewy body dementia (Mollenhauer et al., 2008; Mondello et al., 2014). However, α-synuclein is reported to be elevated in Creutzfeldt–Jacob disease (Kasai et al., 2014; Mollenhauer et al., 2008), traumatic brain injury (Mondello, Buki, Italiano, & Jeromin, 2013), and AD (Slaets et al., 2014). Our finding of increased CSF α-synuclein levels in patients with AD is in accordance with those studies. Furthermore, we found that the α-synuclein levels positively correlated with increased p-tau$_{181}$ in patients with AD. These findings further support the view that the decreased CSF α-synuclein levels can be a marker of synucleinopathies; however, an increase in CSF α-synuclein levels may indicate neurodegeneration irrespective of the underlying neuropathology.

This study has several limitations. The control group was small and mostly composed of women. For ethical reasons, we could not obtain CSF samples from healthy controls; hence, all the correlative data between changes in DMN and CSF biomarker levels were derived from patients with AD. Further studies in a larger sample of both control and patient groups covering prodromal to advanced stages of AD are required. These studies may allow a reliable assessment of the diagnostic power of changes in DMN activity in diagnosing AD compared with CSF biomarkers or other validated biomarkers.

5. Conclusions

The data show that DMN activity changes in AD and is closely related to cognitive functions and Aβ pathology. The findings further indicate that the dorsal PCC and retrosplenial cortices may have special importance in the pathogenesis and cognitive findings of AD.

Disclosure statement

The authors have no actual or potential conflicts of interest.

Acknowledgements

The study was funded by TUBITAK (SBAG 112S360), and is part of the BIOMARKAPD project in the JPND programme.

Appendix A. Supplementary data

Supplementary data associated with this article can be found, in the online version, at http://dx.doi.org/10.1016/j.archger.2015.09.010.

References

Balthazar, M. L., de Campos, B. M., Franco, A. R., Damasceno, B. P., & Cendes, F. (2014). Whole cortical and default mode network mean functional connectivity as potential biomarkers for mild Alzheimer's disease. *Psychiatry Res.*, *221*, 37–42.

Barkhof, F., Haller, S., & Rombouts, S. A. (2014). Resting-state functional mr imaging: a new window to the brain. *Radiology*, *272*, 29–49.

Beckmann, C. F., & Smith, S. M. (2004). Probabilistic independent component analysis for functional magnetic resonance imaging. *IEEE Trans. Med. Imaging*, *23*, 137–152.

Benjamini, Y., & Hochberg, Y. (1995). Controlling the false discovery rate: a practical and powerful approach to multiple testing. *J. R. Stat. Soc.*, *57*(Series B), 289–300.

Blennow, K., Zetterberg, H., & Fagan, A. M. (2012). Fluid biomarkers in alzheimer disease. *Cold Spring Harbor Perspect. Med.*, *2*, a006221.

Buckner, R. L., Snyder, A. Z., Shannon, B. J., LaRossa, G., Sachs, R., Fotenos, A. F., et al. (2005). Molecular, structural, and functional characterization of Alzheimer's disease: evidence for a relationship between default activity, amyloid, and memory. *J. Neurosci.*, *25*, 7709–7717.

Buckner, R. L., Andrews-Hanna, J. R., & Schacter, D. L. (2008). The brain's default network: anatomy, function, and relevance to disease. *Ann. N. Y. Acad. Sci.*, *1124*, 1–38.

Cangoz, B., Karakoc, E., & Selekler, K. (2006). The norm determination and validity–reliability studies of Clock Drawing Test on Turkish Adults and Elderlys (ages 50 and over). *Turk. J. Geriatr.*, *9*, 136–142 (in Turkish).

Celebi, O., Temucin, C. M., Elibol, B., & Saka, E. (2014). Cognitive profiling in relation to short latency afferent inhibition of frontal cortex in multiple system atrophy. *Parkinsonism Relat. Disord.*, *20*, 632–636.

Chhatwal, J. P., Schultz, A. P., Johnson, K., Benzinger, T. L., Jack, C. Jr, Ances, B. M., et al. (2013). Impaired default network functional connectivity in autosomal dominant Alzheimer disease. *Neurology*, *81*, 736–744.

R Core Team (2013). *A language and environment for statistical computing*. Vienna, Austria: R Foundation for Statistical Computing ISBN 3-900051-07-0.

Desgranges, B., Baron, J. C., Lalevee, C., Giffard, B., Viader, F., de La Sayette, V., et al. (2002). The neural substrates of episodic memory impairment in Alzheimer's disease as revealed by fdg-pet: relationship to degree of deterioration. *Brain*, *125*, 1116–1124.

Di, M., artino, A., Scheres, A., Margulies, D. S., Kelly, A. M., Uddin, L. Q., et al. (2008). Functional connectivity of human striatum: a resting state fmri study. *Cereb. Cortex*, *18*, 2735–2747.

Elman, J. A., Madison, C. M., Baker, S. L., Vogel, J. W., Marks, S. M., Crowley, S., et al. (2014). Effects of beta-amyloid on resting state functional connectivity within and between networks reflect known patterns of regional vulnerability. *Cereb. Cortex* .

FEAT (2015). <http://fsl.fmrib.ox.ac.uk/fsl/fslwiki/FEAT> Accessed 01.27.15.

FSL (2015). <http://fsl.fmrib.ox.ac.uk/fsl/> Accessed 01.27.15.

Frings, L., Spehl, T. S., Weber, W. A., Hull, M., & Meyer, P. T. (2013). Amyloid-beta load predicts medial temporal lobe dysfunction in alzheimer dementia Journal of nuclear medicine: official publication. *Soc. Nucl. Med.*, *54*, 1909–1914.

Friston, K. J., Holmes, A. P., Poline, J. B., Grasby, P. J., Williams, S. C., Frackowiak, R. S., et al. (1995). Analysis of fmri time-series revisited. *Neuroimage*, *2*, 45–53.

Gour, N., Felician, O., Didic, M., Koric, L., Gueriot, C., Chanoine, V., et al. (2014). Functional connectivity changes differ in early and late-onset Alzheimer's disease. *Hum. Brain Mapp.*, *35*, 2978–2994.

Greicius, M. D., Srivastava, G., Reiss, A. L., & Menon, V. (2004). Default-mode network activity distinguishes Alzheimer's disease from healthy aging: evidence from functional MRI. *Proc. Natl. Acad. Sci. U. S. A.*, *101*, 4637–4642.

Hahn, K., Myers, N., Prigarin, S., Rodenacker, K., Kurz, A., Forstl, H., et al. (2013). Selectively and progressively disrupted structural connectivity of functional brain networks in Alzheimer's disease—revealed by a novel framework to analyze edge distributions of networks detecting disruptions with strong statistical evidence. *Neuroimage*, *81*, 96–109.

Hardy, J. (1992). An 'anatomical cascade hypothesis' for Alzheimer's disease. *Trends Neurosci.*, *15*, 200–201.

Jack, C. R. Jr, Knopman, D. S., Jagust, W. J., Petersen, R. C., Weiner, M. W., Aisen, P. S., et al. (2013). Tracking pathophysiological processes in Alzheimer's disease: an updated hypothetical model of dynamic biomarkers. *Lancet Neurol.*, *12*, 207–216.

Kasai, T., Tokuda, T., Ishii, R., Ishigami, N., Tsuboi, Y., Nakagawa, M., et al. (2014). Increased alpha-synuclein levels in the cerebrospinal fluid of patients with creutzfeldt-jakob disease. *J. Neurol.*, *261*, 1203–1209.

Koch, W., Teipel, S., Mueller, S., Benninghoff, J., Wagner, M., Bokde, A. L., et al. (2012). Diagnostic power of default mode network resting state fMRI in the detection of Alzheimer's disease. *Neurobiol. Aging*, *33*, 466–478.

Koch, K., Myers, N. E., Gottler, J., Pasquini, L., Grimmer, T., Forster, S., et al. (2014). Disrupted intrinsic networks link amyloid-beta pathology and impaired cognition in prodromal Alzheimer's disease. *Cereb. Cortex* .

Leech, R., & Sharp, D. J. (2014). The role of the posterior cingulate cortex in cognition and disease. *Brain*, *137*, 12–32.

Li, R., Wu, X., Fleisher, A. S., Reiman, E. M., Chen, K., & Yao, L. (2012). Attention-related networks in Alzheimer's disease: a resting functional MRI study. *Hum. Brain Mapp.*, *33*, 1076–1088.

Li, X., Li, T. Q., Andreasen, N., Wiberg, M. K., Westman, E., & Wahlund, L. O. (2013). Ratio of abeta42/p-tau181p in csf is associated with aberrant default mode network in ad. *Sci. Rep.*, *3*, 1339.

Margulies, D. S., Kelly, A. M., Uddin, L. Q., Biswal, B. B., Castellanos, F. X., & Milham, M. P. (2007). Mapping the functional connectivity of anterior cingulate cortex. *Neuroimage*, *37*, 579–588.

McKhann, G., Drachman, D., Folstein, M., Katzman, R., Price, D., & Stadlan, E. M. (1984). Clinical diagnosis of Alzheimer's disease: report of the nincds-adrda work group under the auspices of department of health and human services task force on Alzheimer's disease. *Neurology*, *34*, 939–944.

McKhann, G. M., Knopman, D. S., Chertkow, H., Hyman, B. T., Jack, C. R. Jr., Kawas, C. H., et al. (2011). The diagnosis of dementia due to Alzheimer's disease: recommendations from the National Institute on Aging-Alzheimer's Association workgroups on diagnostic guidelines for Alzheimer's disease. *Alzheimers Dement.*, *7*, 263–269.

Mollenhauer, B., Cullen, V., Kahn, I., Krastins, B., Outeiro, T. F., Pepivani, I., et al. (2008). Direct quantification of csf alpha-synuclein by elisa and first cross-sectional study in patients with neurodegeneration. *Exp. Neurol.*, *213*, 315–325.

Mondello, S., Buki, A., Italiano, D., & Jeromin, A. (2013). Alpha-synuclein in csf of patients with severe traumatic brain injury. *Neurology*, *80*, 1662–1668.

Mondello, S., Constantinescu, R., Zetterberg, H., Andreasson, U., Holmberg, B., & Jeromin, A. (2014). Csf alpha-synuclein and uch-l1 levels in Parkinson's disease and atypical parkinsonian disorders. *Parkinsonism Relat. Disord.*, *20*, 382–387.

Pengas, G., Williams, G. B., Acosta-Cabronero, J., Ash, T. W., Hong, Y. T., Izquierdo-Garcia, D., et al. (2012). The relationship of topographical memory performance to regional neurodegeneration in alzheimer's disease. *Front. Aging Neurosci.*, *4* (17) .

Rektorova, I. (2014). Resting-state networks in Alzheimer's disease and Parkinson's disease. *Neuro-Degenerative Dis.*, *13*, 186–188.

Saka, E., Mihci, E., Topcuoglu, M. A., & Balkan, S. (2006). Enhanced cued recall has a high utility as a screening test in the diagnosis of Alzheimer's disease and mild cognitive impairment in turkish people. *Arch. Clin. Neuropsychol.*, *21*, 745–751.

Selkoe, D. J. (2002). Deciphering the genesis and fate of amyloid beta-protein yields novel therapies for alzheimer disease. *J. Clin. Investig.*, *110*, 1375–1381.

Sheline, Y. I., Morris, J. C., Snyder, A. Z., Price, J. L., Yan, Z., D'Angelo, G., et al. (2010). Apoe4 allele disrupts resting state fmri connectivity in the absence of amyloid plaques or decreased csf abeta42. *J. Neurosci.*, *30*, 17035–17040.

Sperling, R. A., Laviolette, P. S., O'Keefe, K., O'Brien, J., Rentz, D. M., Pihlajamaki, M., et al. (2009). Amyloid deposition is associated with impaired default network function in older persons without dementia. *Neuron*, *63*, 178–188.

Sperling, R. A., Jack, C. R. Jr., Black, S. E., Frosch, M. P., Greenberg, S. M., Hyman, B. T., et al. (2011). Amyloid-related imaging abnormalities in amyloid-modifying therapeutic trials: recommendations from the Alzheimer's association research roundtable workgroup. *Alzheimers Demen.*, *7*, 367–385.

Statistical Parametric Mapping SPM Software (2015). <http://www.fil.ion.ucl.ac.uk/spm/software/spm8/> Accessed 01.27.15.

Vann, S. D., Aggleton, J. P., & Maguire, E. A. (2009). What does the retrosplenial cortex do? *Nat. Rev. Neurosci.*, *10*, 792–802.

Wang, L., Brier, M. R., Snyder, A. Z., Thomas, J. B., Fagan, A. M., Xiong, C., et al. (2013). Cerebrospinal fluid abeta42, phosphorylated tau181, and resting-state functional connectivity. *JAMA Neurol.*, *70*, 1242–1248.

del Campo, M., Mollenhauer, B., Bertolotto, A., Engelborghs, S., Hampel, H., Simonsen, A. H., et al. (2012). Recommendations to standardize preanalytical confounding factors in Alzheimer's and Parkinson's disease cerebrospinal fluid biomarkers: an update. *Biomarkers Med.*, *6*, 419–430.

Slaets, S., Vanmechelen, E., Le Bastard, N., Decraemer, H., Vandijck, M., Martin, J. J., et al. (2014). Increased csf alpha-synuclein levels in Alzheimer's disease: correlation with tau levels. *Alzheimers Demen.*, *10*(Suppl. 5), S290–8.